

THE EVOLUTION OF GALAXY CLUSTERING SINCE $z = 1$

S.PHLEPS¹, K.MEISENHEIMER¹

¹*Max-Planck-Institut für Astronomie, Königstuhl 17, 69121 Heidelberg, Germany*

Abstract. We present results of an investigation of clustering evolution of field galaxies between a redshift of $z \sim 1$ and the present epoch. The current analysis relies on a sample of ~ 3600 galaxies from the **C**alar **A**lto **D**eep **I**maging **S**urvey (CADIS). The multicolor classification and redshift determination is reliable up to $I = 23^{mag}$. The redshift distribution extends to $z \sim 1.1$, the resolution is $\Delta cz = 12000 \text{ km s}^{-1}$. Thus the amplitude of the three-dimensional correlation function has to be estimated by means of the projected correlation function $w(r_p)$. The validity of the deprojection was tested on the Las Campanas Redshift Survey (LCRS). The LCRS also serves as "local" measurement. We invented a new method to overcome the influence of redshift errors on $w(r_p)$. For evolution of the clustering strength the ansatz $\xi(r_{com}, z) \propto (1+z)^q$ is used. For the galaxies as a whole the evolution parameter turns out to be $q \approx -1.9$, according to the prediction of linear theory. A formal dependency on the cosmology is presumably due to the small number of fields observed. However, the measured clustering growth clearly depends on Hubble type. At $z \sim 1$ early type galaxies are already much stronger clustered, an increase with $q \simeq -1$ is sufficient to explain the present day amplitude of the correlation function.

1 The Calar Alto Deep Imaging Survey

CADIS combines a very deep emission line survey carried out with an imaging Fabry-Perot interferometer with a deep multicolour survey using three broad-band optical to NIR filters and up to thirteen medium-band filters when fully completed. The combination of different observing strategies facilitates not only the detection of emission line objects but also the derivation of photometric spectra of all objects in the fields without performing time consuming slit spectroscopy.

For the multicolor sample, a classification scheme was developed, which is based on template spectral energy distributions (*SEDs*) [5]. The classification algorithm basically compares the observed colors of each object with a color library of known objects. This color library is assembled from observed spectra by synthetic photometry performed on an accurate representation of the instrumental characteristics used by CADIS. Using the minimum variance estimator, each object is assigned a type (star – QSO – galaxy), a redshift (if it is not classified as star), and an *SED* (in terms of a number, $0 \equiv \text{E0}$, $100 \equiv \text{starburst}$). The formal errors in this process depend on magnitude and type of the object and are of the order of $\sigma_z = 0.017$, and $\sigma_{SED} = 2$, respectively.

The seven CADIS fields measure $\approx 1/30^\circ$ each and are located at high Galactic latitude to avoid dust absorption and reddening. Four of these have been fully analysed so far. We identified 3626 galaxies with $I \leq 23$ in the redshift range $0.2 \leq z \leq 1.07$.

2 The projected correlation function

The projected correlation function $w(r_p)$ was first introduced by [1] to overcome the influence of non-negligible peculiar velocities on the three-dimensional correlation function. Redshift inaccuracies also increase the noise and suppress the correlation signal. Therefore we used the projected correlation function to investigate the evolution of galaxy clustering. It is defined by

$$\begin{aligned} w(r_p) &= 2 \int_0^\infty \xi \left[(r_p^2 + \pi^2)^{1/2} \right] d\pi \\ &= 2 \int_{r_p}^\infty \xi(r) (r^2 - r_p^2)^{-1/2} r dr . \end{aligned} \quad (1)$$

r_p is the projected distance between pairs of galaxies (the distance perpendicular to the line of sight), π is the distance between the two galaxies parallel to the line of sight, and $r^2 = r_p^2 + \pi^2$. If $\xi(r) = (r/r_0)^{-\gamma}$, then equation (1) yields

$$w(r_p) = Cr_0^\gamma r_p^{1-\gamma} \quad (2)$$

with

$$C = \sqrt{\pi} \frac{\Gamma((\gamma - 1)/2)}{\Gamma(\gamma/2)}, \quad (3)$$

Thus computing $w(r_p)$ provides a measurement of the parameters of the three-dimensional correlation function, namely r_0 and γ .

Following [1] one can calculate the projected correlation function from

$$w(r_p) = \int_{-\delta\pi}^{+\delta\pi} \xi(r_p, \pi) d\pi. \quad (4)$$

Since the three-dimensional two-point correlation function has the form of a power law, it converges rapidly to zero with increasing pair separation. Therefore the integration limits do not have to be $\pm\infty$, they only have to be large enough to include all correlated pairs. Since the observable in the first place is the redshift z instead of the physical separation, we make a coordinate transform [3]:

$$w(r_p) = \int_{-\delta z}^{+\delta z} \xi(r_p, \pi) \frac{c}{H_0(1+z)^2 \sqrt{1+2q_0 z}} dz, \quad (5)$$

for $\Omega_\Lambda = 0$.

The way to estimate $w(r_p)$ in practice is to count the projected distances between pairs of galaxies that are separated in redshift space by not more than δz , in appropriate projected distance bins. We use the estimator by [2], which we will call $\zeta_{esti}(r_p)$ in the following. To derive $w(r_p)$, $\zeta_{esti}(r_p)$ has to be multiplied with the "effective depth" Δr_\parallel in which galaxies are taken into account.

In reality, one has to cope with a selection function of some kind or another, and not with a top-hat function (of probability unity to find a galaxy within the borders of the survey and zero otherwise). The varying probability to find pairs of galaxies separated by a redshift δz within the survey has to be taken into account. It can be included in the calculation by multiplying the integrand in equation (6) with the squared redshift distribution, normalised to unity at its maximum. With this correction for the selection function, the "depth" converges to a fixed value for $\delta cz \rightarrow \infty$ and does not grow anymore, even if the integration limits cover more than the total depth of the survey, thus

$$\begin{aligned} w(r_p) &= \zeta_{esti}(r_p) \cdot \Delta r_\parallel \\ &= \zeta_{esti} \cdot \int_{-\delta z}^{+\delta z} \left[\frac{1}{N_z} \frac{dN}{dz} \right]^2 \frac{c dz}{H_0(1+z)^2 \sqrt{1+2q_0 z}} \end{aligned} \quad (6)$$

for $\Omega_\Lambda = 0$.

The choice of the integration limit δz is somewhat arbitrary. To find the appropriate integration limits, we simulated the influence of redshift errors on the projected correlation function. We added artificial redshift errors to redshifts of LCRS galaxies. The errors (one time for a resolution of $\Delta cz = 5000 \text{ km s}^{-1}$ and the other time with $\Delta cz = 12000 \text{ km s}^{-1}$, the size of the CADIS redshift resolution) were randomly drawn out of a Gaussian error distribution. We calculated the projected correlation function for the modified samples for increasing integration limits δcz . The amplitude was fitted at $r_p = 500h^{-1} \text{ kpc}$, in the range $-1.15 \leq \log r_p \leq -0.3$, to make sure we fit it where the signal to noise is high. Also the choice of $r_p = 500h^{-1} \text{ kpc}$ facilitates the comparison with the CADIS data, where we fit the amplitude at $r_p \approx 316h^{-1} \text{ kpc}$ (at the mean redshift of the survey (\bar{z}) this corresponds to a comoving separation of $\approx 505h^{-1} \text{ kpc}$).

Figure 1 shows the amplitude of $w(r_p = 500h^{-1} \text{ kpc})$, for increasing integration limits. The measurement is compared to the modified data.

One starts to sample the correlation signal when the integration limits are larger than the full width at half maximum of the redshift error distribution. Also the amplitude is diminished. For errors of

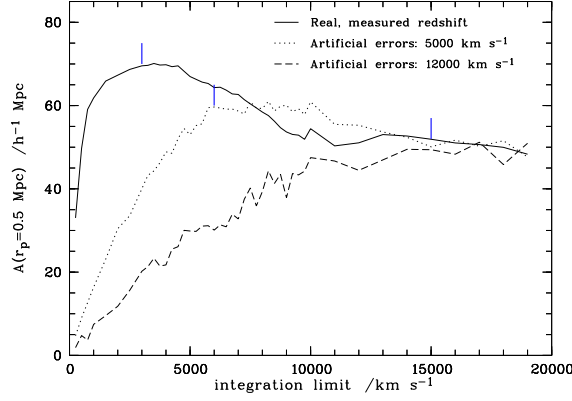


Figure 1: The influence of redshift measurement errors on the projected two-point correlation function, shown is the weighted mean of four sectors. $w(r_p)$ for increasing integration limits is calculated for an $\Delta cz = 5000 \text{ km s}^{-1}$ (dotted line), and for $\Delta cz = 12000 \text{ km s}^{-1}$ (dashed line). The errors of the fits are not plotted here to avoid confusion. The marks indicate the integration limits which have to be chosen for the calculation of $w(r_p)$.

$\Delta cz = 12000 \text{ km s}^{-1}$, the maximum amplitude is a factor 1.4 lower than in the case of the unchanged data.

We calculated $w(r_p)$ for the CADIS data with $\pm \delta cz = 15000 \text{ km s}^{-1}$. To facilitate the direct comparison with the LCRS data, we used the modified sample (with artificial errors of size $\Delta cz = 12000 \text{ km s}^{-1}$) and the same integration limits.

Bright stars in our field were masked out, and a random catalogue consisting of 10000 "galaxies" was generated with the same properties as the real data. The calculation was carried out for a closed high-density model ($\Omega_0 = 1, \Omega_\Lambda = 0$), a hyperbolic low-density model ($\Omega_0 = 0.2, \Omega_\Lambda = 0$), and a flat low-density model with non-zero comological constant ($\Omega_0 = 0.3, \Omega_\Lambda = 0.7$). Figure 2 shows the results for the latter two ones.

From the amplitude of $w(r_p)$ we can deduce the amplitude of the three-dimensional correlation func-

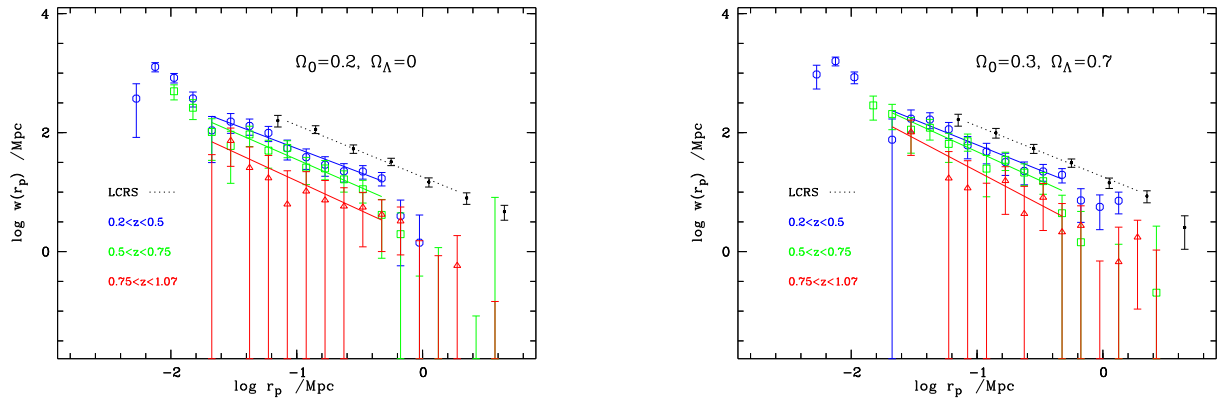


Figure 2: Projected correlation function in three redshift bins, for an open model (left panel), and for a flat universe with a non-zero cosmological constant (right panel).

tion at $r_{com} = 1h^{-1} \text{ Mpc}$:

With $\xi(r) = (r/r_0)^{-\gamma}$

$$\begin{aligned} \xi(r = 1\text{Mpc}) &= r_0^\gamma \\ w(r_p) &= Cr_p^{1-\gamma} r_0^\gamma \\ &= Cr_p^{1-\gamma} \xi(r = 1\text{Mpc}) \end{aligned}$$

$$\Rightarrow \xi(r_{com} = 1\text{Mpc}) = \frac{w(r_p)(1+z)^\gamma}{Cr_p^{1-\gamma}}, \quad (7)$$

with the numerical factor C from equation (3).

We can now parametrise the evolution with a parameter q which gives directly the deviation from the global Hubble flow:

$$\xi(r_{com} = 1\text{Mpc}) = \xi_0(1+z)^q. \quad (8)$$

q can be deduced straightforwardly: if one fits $\log \xi(r_{com} = 1\text{Mpc})$ versus $\log(1+z)$, it is just the slope of the straight line.

We find $q = -2.68 \pm 0.16$ for $\Omega_0 = 1$, $\Omega_\Lambda = 0$, $q = -1.92 \pm 0.17$ for $\Omega_0 = 0.2$, $\Omega_\Lambda = 0$, and $q = -1.23 \pm 0.20$ for $\Omega_0 = 0.3$, $\Omega_\Lambda = 0.7$. The formal dependence on the cosmological model adopted for the calculation is larger than expected from a simple examination of the distances corresponding to a certain angle θ . Therefore we regard this as an indication that the differences are presumably due to the small number of fields observed.

We can compare our results for the $\Omega_0 = 1$, $\Omega_\Lambda = 0$ case with the results of [3]. For the direct comparison we have to multiply our measured amplitudes of the projected correlation function by 1.4 to correct for the influence of large redshift errors.

With this correction, the CFRS data points are consistent with our own measurement, although with large errors, see Figure 3. [3] claim that if $r_0(z=0) = 5h^{-1}$ Mpc, $0 < \epsilon \lesssim 2$. The fit of their data points, including the connection to $z=0$, yields $q = -3.043 \pm 0.213$ ($\cong \epsilon = 1.8$). If the connection to $z=0$ is disregarded, we find $q = -1.184 \pm 0.634$. The fit including our redshift error corrected LCRS point instead of the [4] point yields $q = -2.298 \pm 0.238$. This is even a bit less than our own measurement ($q = -2.68 \pm 0.16$), but nevertheless equal within the errors.

2.1 The evolution of clustering for different Hubble types

Our multicolor classification scheme gives the *SED* of each galaxy, and thus we are able to calculate the projected correlation function for different Hubble types. We divided our sample at $SED = 60$, the sample with $0 \leq SED \leq 60$ is called "early type", and the sample with $60 < SED \leq 100$ is called "late type" in the following. The amplitudes of the correlation function of the early type galaxies are at all redshifts significantly larger than for the late type ones, and also clearly larger than for the complete CADIS sample. Also the evolution of the clustering strength is different. The amplitude of the correlation function of the early type galaxies evolves much slower, we find $q = -1.71 \pm 0.39$ for $\Omega_0 = 1$, $\Omega_\Lambda = 0$, $q = -1.37 \pm 0.36$ for $\Omega_0 = 0.2$, $\Omega_\Lambda = 0$, and $q = -0.67 \pm 0.33$ for $\Omega_0 = 0.3$, $\Omega_\Lambda = 0.7$. For the late type sample the errors are too large to facilitate a quantitative statement about the clustering evolution.

Combining *SED* and redshift information, we are able to calculate restframe B band luminosities for all the galaxies. Therefore we divided our sample at $M_B = -18^{mag}$, and calculated the projected correlation function for bright and faint galaxies in the redshift range $0.3 \leq z \leq 0.6$, where the number of faint galaxies is sufficient to enable the determination of the amplitude of the projected correlation function. The bright galaxies are clearly higher clustered than the faint ones. Figure 3 shows the amplitudes of the three-dimensional correlation function and the fit for the evolution parameter q for the complete sample, for early and late type galaxies and also for the bright and the faint sample. The left panel shows the results for $\Omega_0 = 0.3$, $\Omega_\Lambda = 0.7$, the right panel shows the comparison of our data with the CFRS data.

3 Conclusion

We find that the amplitude of the correlation function of all the galaxies in our sample grows with $q \simeq -1.9$ between a redshift of $z \approx 1.1$ and the present epoch. The rate of clustering growth is consistent with the results of linear perturbation theory ($q = -2$). The amplitude of the early type galaxies grows much slower with redshift ($q \simeq -1$). This result can be explained in the context of biased galaxy formation, if we assume a substantial evolution of the galaxies between a redshift of $z \approx 1.1$ and today. The first generation of galaxies forms in a highly clustered state, in the bumps and wiggles superimposed on the very large scale perturbations of the dark matter density field, whereas the next generations of galaxies form later in the lower clustered environment in the wings of the super large scale overdensities. Therefore early type galaxies are much stronger clustered than the young,

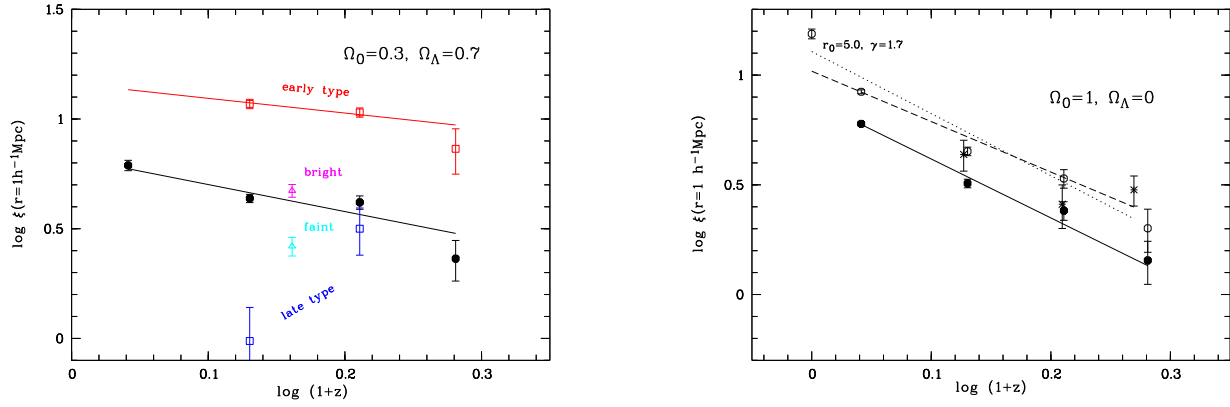


Figure 3: The evolution of the clustering strength (at $1h^{-1}$ Mpc) with redshift. Left panel: The line is the fit to the data points, the first data point is the weighted mean of four LCRS sectors, the three other ones are CADIS data, for a flat universe with a non-zero cosmological constant. The LCRS point is not included in the fit for the early type galaxies. Right panel: The amplitudes of the three dimensional correlation function at $r_{com} = 1h^{-1}$ Mpc, deduced from the projected correlation function of the CFRS data (crosses), in comparison with our own data (filled symbols). The open symbols are our data points corrected for the influence of the redshift errors on the amplitude of the projected correlation function. The dotted line is the fit of the CFRS data points including the value of $r_0(z=0)$ from [4], the dashed line is the fit using the corrected LCRS point instead.

late type ones even at higher redshifts. While the universe evolves and the clustering of the underlying dark matter density field grows, galaxies age, and eventually merge to form massive ellipticals. They add to the early type population at different times, thus the early type sample consists of galaxies of different ages, which have formed in increasingly less clustered states. This means that biasing decreases with increasing redshift. The net effect is a very slow growth of clustering of early type galaxies.

Merging also plays an important role, because of two effects on the correlation function: first of all, galaxies change their *SEDs* on relatively small timescales. They "suddenly" disappear from the lower clustered late type sample and reappear in the early type sample. The second effect is that while two galaxies merger to form one, the small distances disappears, the probability of finding a galaxy near another galaxies decreases, and therefore the amplitude of the correlation function decreases.

If bright galaxies form in the highest peaks of the dark matter field, they are expected to be higher clustered than the faint ones. The difference in clustering strength is larger for the early type/late type sample than for bright and faint galaxies, which corroborates the hypothesis, that galaxy evolution and merging plays an important role in the evolution of clustering.

References

- [1] Davis, M. and Peebles, P., 1983, ApJ 267, 465
- [2] Landy, S. D. and Szalay, A. S., 1993, ApJ 412, 64
- [3] Le Fevre, O. et al., 1996, ApJ 461, 534
- [4] Loveday, J. et al., 1995 ApJ 442, 457
- [5] Wolf, C. et al., 2001, A&A 365, 681